Stem Cell Reports

Article

ISSCR

OPEN ACCESS

Boundary Caps Give Rise to Neurogenic Stem Cells and Terminal Glia in the Skin

Aurélie Gresset,[1,4] Fanny Coulpier,[1,4] Gaspard Gerschenfeld,[1,3] Alexandre Jourdon,[1,3] Graziella Matesic,[1] Laurence Richard,[2] Jean-Michel Vallat,[2] Patrick Charnay,[1,*] and Piotr Topilko[1]

[1]Ecole Normale Supérieure, Institut de Biologie de l'ENS (IBENS), and INSERM U1024, and Centre National de la Recherche Scientifique (CNRS) UMR 8197, Paris 75005, France
[2]National Reference Centre "Rare Peripheral Neuropathies" Department of Neurology, Centre Hospitalier Universitaire de Limoges, 87042 Limoges, France
[3]Sorbonne Universités, UPMC Université Paris 06, IFD, 4 Place Jussieu, 75252 Paris Cedex 05, France
[4]Co-first author
*Correspondence: patrick.charnay@ens.fr
http://dx.doi.org/10.1016/j.stemcr.2015.06.005

SUMMARY

While neurogenic stem cells have been identified in rodent and human skin, their manipulation and further characterization are hampered by a lack of specific markers. Here, we perform genetic tracing of the progeny of boundary cap (BC) cells, a neural-crest-derived cell population localized at peripheral nerve entry/exit points. We show that BC derivatives migrate along peripheral nerves to reach the skin, where they give rise to terminal glia associated with dermal nerve endings. Dermal BC derivatives also include cells that self-renew in sphere culture and have broad in vitro differentiation potential. Upon transplantation into adult mouse dorsal root ganglia, skin BC derivatives efficiently differentiate into various types of mature sensory neurons. Together, this work establishes the embryonic origin, pathway of migration, and in vivo neurogenic potential of a major component of skin stem-like cells. It provides genetic tools to study and manipulate this population of high interest for medical applications.

INTRODUCTION

The neural crest (NC) is an embryonic, multipotent cell population that migrates extensively through the periphery and gives rise to various cell lineages, including most of the glial and neuronal components of the peripheral nervous system (PNS). NC cell settlement is normally accompanied by restriction to particular cell fates (Le Douarin and Dupin, 2003). However, recent studies have identified stem cell-like populations within adult NC targets, which show developmental potentials resembling those of NC cells (Dupin and Sommer, 2012; Le Douarin and Dupin, 2003). Among these populations, adult multipotent skin stem cells have attracted particular attention because they are easy to access, which would facilitate their use in regenerative medicine.

Fate-mapping studies have revealed the existence of different types of trunk skin stem cell populations that possess neurogenic and gliogenic potential, with both NC and non-NC origins. Stem cells confined to the dermal papillae of hair follicles originate from the mesoderm, whereas populations restricted to the glial and melanocyte lineages are derived from the NC (Dupin and Sommer, 2012; Jinno et al., 2010; Wong et al., 2006). These different cell populations can be cultured as floating spheres and generate neurons and Schwann cells under differentiation conditions (Biernaskie et al., 2006; Wong et al., 2006). However, a lack of specific markers has prevented their detailed localization and further characterization and purification.

Another type of NC-derived stem cell-like population has been identified in the embryo at the interface between the CNS and PNS. These cells form the so-called boundary caps (BCs), which are transiently observed at the nerve root entry/exit points along the neural tube (Niederländer and Lumsden, 1996). Fate analyses, taking advantage of BC-specific expression of the *Krox20* (also known as *Egr2*) transcription factor gene and available knockins at this locus (Vermeren et al., 2003; Voiculescu et al., 2000), have established that BC cells give rise to the Schwann cell component of the nerve roots and, in the dorsal root ganglia (DRGs), to nociceptive neurons as well as glial satellite cells (Maro et al., 2004). Furthermore, in culture, BC cells can generate Schwann cells, myofibroblasts, astrocytes, and neurons (Zujovic et al., 2011), and, when grafted into the lesioned spinal cord, efficiently migrate toward the lesion and differentiate into functional myelinating Schwann cells (Zujovic et al., 2010). Together, these studies indicate that BC cells have a broad differentiation potential and suggest that they constitute multipotent stem cells in the embryo.

These fate analyses relied on the restriction of *Krox20* expression to BC cells during early PNS development. However, from embryonic day 15.5 (E15.5), *Krox20* also is expressed in Schwann cells (Topilko et al., 1994), thereby preventing later analysis of BC derivatives. To circumvent this problem, we have generated a Cre recombinase knockin in a novel BC-specific marker, *Prss56,* previously known as *L20* (Coulpier et al., 2009), and we used it to trace
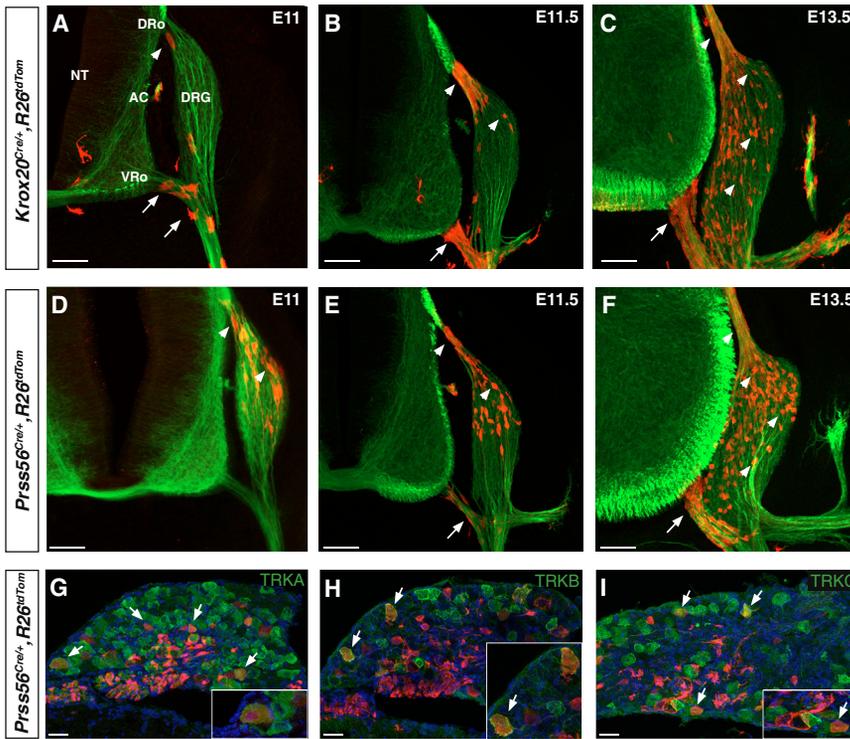
Figure 1. Tracing of *Krox20*- and *Prss56*-Expressing BC Cells along the Nerve Roots and in the DRG

(A–F) Transverse sections of $Krox20^{Cre/+}$, $R26^{tdTom}$ (A–C) and $Prss56^{Cre/+}$,$R26^{tdTom}$ (D–F) embryos, between E11 and E13.5 as indicated, were analyzed by immunocytochemistry using antibodies against tdTOM (red) and βIII-tubulin (green). Arrows and arrowheads indicate ventral and dorsal BC derivatives, respectively.

(G–I) Sections through the DRG from E18.5 $Prss56^{Cre/+}$,$R26^{tdTom}$ embryos were analyzed by immunocytochemistry using antibodies against tdTOM (red) and neuronal markers (TRKA, TRKB, and TRKC, green), as indicated. Insets show higher magnifications of the corresponding figures.

NT, neural tube; DRo, dorsal root; VRo, ventral root; AC, accessory nerve; DRG, dorsal root ganglion. Scale bars, 100 μm (A–F) and 50 μm (G–I). See also Figure S2.

BC cell derivatives in the embryo and the adult. *Prss56* encodes a trypsin-like serine protease and its mutation in the retina has been associated with microphtalmia in humans and mice (Nair et al., 2011). In this study, we show that, during embryogenesis, some of the BC derivatives rapidly migrate along the peripheral nerves and settle in the skin, where they provide terminal glia as well as multipotent progenitors that have broad differentiation capacities in culture and after transplantation into adult mice. This work, therefore, reveals the embryonic origin, pathway of migration, and in vivo neurogenic potential of a multipotent stem cell-like population in the skin.

RESULTS

Dorsal BC Cells Are Heterogeneous and Give Rise to the Different Neuronal Subtypes in the DRGs

Analysis of *Prss56* expression by in situ hybridization on whole embryos indicated that it is restricted to BC cells between E10.5 and E13.5 (Coulpier et al., 2009; Figures S1A, S1B, S3A, and S3B). Furthermore, apart from BC cells, no expression was detected outside of the CNS until E17.5 (Coulpier et al., 2009). On this basis, we generated a Cre knockin in *Prss56* to perform BC derivative tracing studies (Figure S1C). The pattern of expression of *Prss56* was not affected in heterozygous mutants, whereas *Prss56* mRNA

was completely absent from homozygous mutants (Figures S1B and S1D), indicating that the mutation represents a null allele for *Prss56*. Homozygous mutant animals did not show any obvious phenotype in the PNS.

In an initial series of experiments, we compared expression and tracing patterns obtained with the *Prss56* and *Krox20* markers. To this end, we first performed in situ hybridization for *Prss56* mRNA on $Krox20^{lacZ}$ knockin embryos, in which β-galactosidase activity faithfully recapitulates *Krox20* expression (Maro et al., 2004). We found that, between E11.5 and E13.5, *Krox20* and *Prss56* showed overlapping patterns of expression at the levels of both dorsal and ventral roots (Figure S2A). To compare the progeny of *Krox20*- and *Prss56*-expressing BC cells, we combined the $Krox20^{Cre}$ (Voiculescu et al., 2000) or $Prss56^{Cre}$ alleles with the $R26^{tdTom}$ locus, in which Cre recombination leads to permanent activation of the tandem dimer tomato (tdTom) fluorescent reporter (Madisen et al., 2010; Figure S1E). We searched for labeled cells in the nerve roots and DRGs between E11 and E13.5. Using the $Krox20^{Cre}$ driver, we confirmed that the first traced cells appeared in the ventral root before E11 (Figure 1A; Coulpier et al., 2009), whereas labeled cells appeared in the dorsal root around that stage and in the DRGs later on (Figures 1A–1C; Maro et al., 2004). In contrast, in $Prss56^{Cre/+}$,$R26^{tdTom}$ embryos, the first labeled cells appeared in the dorsal root and in the dorsal part of the DRGs around E11 (Figure 1D).

Labeled cells along the ventral root only appeared at later stages (Figures 1E and 1F). In the nerve roots, labeled cells from both tracing systems gave rise to SOX10-positive Schwann cell precursors (Figure S2B; Maro et al., 2004). Similarly, in the DRGs, both types of traced cells gave rise to putative neurons with extending axons (Figure S2C).

Neurogenesis in the DRGs involves two phases, with mechanoceptive and proprioceptive neurons emerging first, followed by nociceptors (Marmigère and Ernfors, 2007). We have shown previously that the only neurons generated by *Krox20*-expressing BC cells in the DRGs are nociceptors (Maro et al., 2004). To identify the neuronal derivatives of the *Prss56*-expressing BC cell population, we analyzed DRG sections from E18.5 $Prss56^{Cre/+}, R26^{tdTom}$ embryos by co-immunostaining them with antibodies against the tracer tdTOM and TRKA (nociceptive), TRKB (mechanoceptive), or TRKC (proprioceptive) neurotrophic receptors. We found that traced cells included all three types of neurons (Figures 1G–1I). Quantification indicated that they represented 9.8% ± 1.9%, 6.3% ± 2.8%, and 13.3% ± 4.6% of the TRKA-, TRKB-, and TRKC-positive neuronal populations, respectively. The observation of mechanoceptive and proprioceptive neurons among BC derivatives traced with the *Prss56* driver is consistent with the presence of traced cells in the DRGs from E11 (Figure 1D), when these neuronal types are generated (Marmigère and Ernfors, 2007). In double-traced $Krox20^{Cre/+}$, $Prss56^{Cre/+}, R26^{tdTom}$ embryos, labeled cells represented 9.2% ± 1.1% of the TRKA-positive neurons. This proportion is similar to those obtained with each tracing individually, suggesting that *Krox20*- and *Prss56*-expressing BC cell populations overlap.

Together, these data suggest the existence of heterogeneity within BC cells, with *Krox20* and *Prss56* being expressed in distinct, although overlapping subpopulations. In contrast to what was thought previously, dorsal BC cells give rise to the different neuronal subtypes in the DRGs.

Ventral Root BC Derivatives Migrate along the Peripheral Nerves to the Skin

We noticed that, from E11.5 in $Prss56^{Cre/+}, R26^{tdTom}$ embryos, some labeled cells were located in the proximal part of the ventral ramus (VR) (Figure 2A), suggesting that the migration of ventral BC derivatives may extend beyond the root. To investigate this possibility, we immunostained transverse sections from $Prss56^{Cre/+}, R26^{tdTom}$ embryos at brachial, thoracic, and lumbar levels for tdTOM and βIII-tubulin, a neuronal/axonal marker, at successive stages of development (Figure 2). At E11.5, labeled cells were present in the ventral root and in the proximal part of the VR of all spinal nerves (Figure 2A). At E11.75, labeled cells had accumulated in the distal part of the elongating VR and a few traced cells were detected in the proximal segment of the

growing dorsal ramus (DR) (Figure 2B). At E12–E12.5, sparse labeled cells were present along the extending spinal nerves (Figures 2C and 2D). From E12.5–E13, labeled cells were observed at the level of the skin (Figures 2D and 2E). Subsequently, their number considerably increased in the cutaneous nerves in both the dorsal (Figure 2F) and ventral (Figure 2G) skin. From these stages, labeled cells were concentrated at both extremities of the somatosensory nerves (root and cutaneous segments) and had almost disappeared from the central segments (Figures 2F and 2G).

The spatial-temporal distribution of the labeled cells along spinal nerves suggests a wave of migration from the BCs to the skin along the peripheral nerves, between E11.5 and E13. To rule out the possibility that some cells in the skin might activate *Prss56* de novo, we performed in situ hybridization and RT-PCR analyses on skin preparations at E13.5, when a large number of labeled cells had accumulated in the skin. At this stage, *Prss56* mRNA was restricted to the BCs and was not detected in the skin by either procedure (Figures S3A–S3C). These results further support the idea that the labeled skin cells are derived from the BCs by migration along the nerves.

Skin BC Derivatives Include Different Types of Schwann-like Cells

To investigate the distribution and identity of BC derivatives in the trunk skin after birth, we first performed a whole-mount immunohistochemistry analysis of $Prss56^{Cre/+}$, $R26^{tdTom}$ newborn dorsal skin preparations, staining for tdTOM and βIII-tubulin. This revealed a dense network of traced cells exclusively associated with the nerves in the hypodermis and dermis (Figure 3A). In the subcutaneous nerves, some of the traced cells expressed the myelin marker MBP (Figure 3B), indicating that they were myelinating Schwann cells.

Staining of transverse sections for βIII-tubulin and PGP9.5, an axonal marker present in terminal endings, confirmed the systematic association of the labeled cells with dermal nerves (Figures 3C and 3D). In the dermis, these traced cells were positive for the marker P75[NGFR] (Figure 3E), which is expressed in NC-derived, embryonic and adult stem cells and in immature and adult, non-myelinating Schwann cells (Jessen et al., 2015). In addition, they expressed the Schwann cell marker S100 (Figure 3F), but not the myelin marker MBP (Figure 3B), and were, therefore, immature/non-myelinating Schwann cells. They could be classified into three categories as follows: (1) those associated with dermal nerve fibers (Figures 3A and 3E, closed arrows), (2) lanceolate endings around hair follicles (Figures 3C, 3D, and 3F, empty arrowheads), and (3) free nerve endings of nociceptive fibers (Figures 3C, 3D, and 3G, closed arrowheads). Lanceolate endings are circumferential structures that surround the hair follicle and are composed of
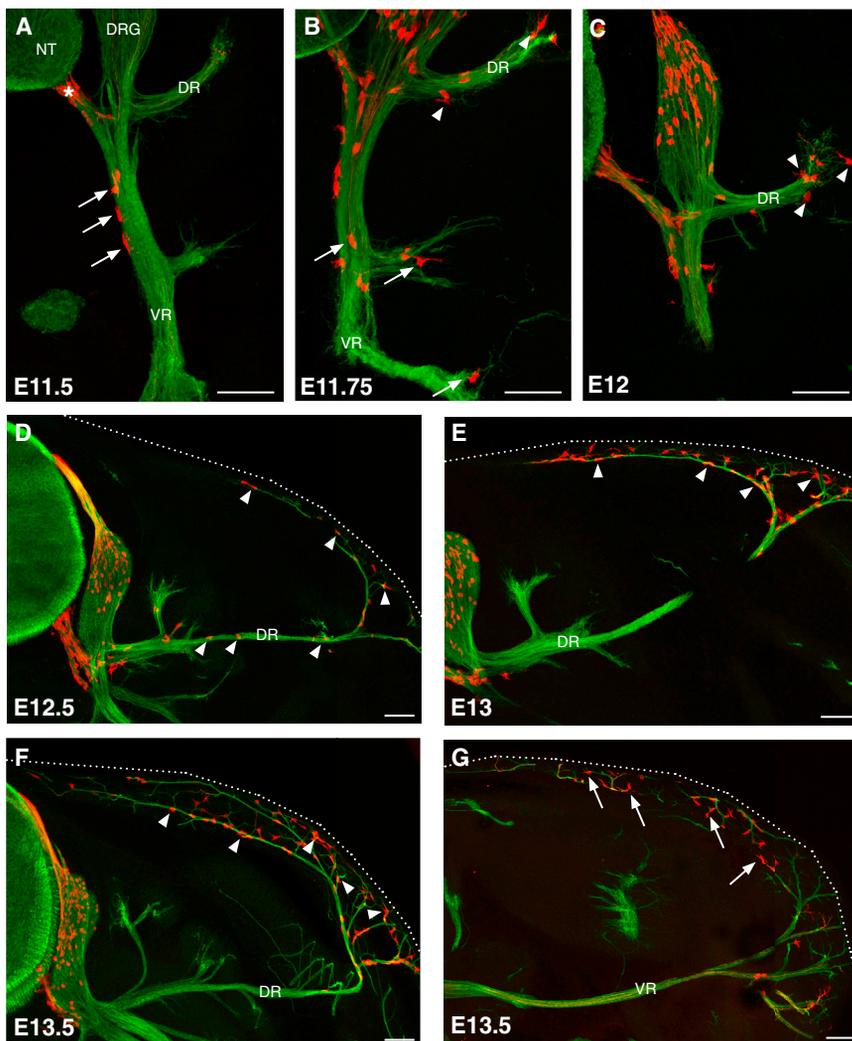
Figure 2. BC Derivatives Migrate along the Peripheral Nerves to the Skin

Transverse sections through the trunk of $Prss56^{Cre/+},R26^{tdTom}$ embryos, between E11.5 and E13.5 as indicated, were analyzed by immunocytochemistry using antibodies against tdTOM (red) and βIII-tubulin (green).

(A) At E11.5, tdTOM-positive cells are present along the ventral nerve root (asterisk) and the proximal part of the ventral ramus (VR) (arrows).

(B and C) Between E11.75 and E12, traced cells are detected along the VR (arrows) and the extending dorsal ramus (DR) (arrowheads).

(D) At E12.5, isolated traced cells are present along the entire trajectory of the nerve (arrowheads).

(E–G) From E13, tdTOM-positive cells are observed at cutaneous nerves in the dorsal (arrowheads) and ventral (arrows) skin. Dotted lines mark the embryo.

NT, neural tube; DRG, dorsal root ganglia. Scale bars, 100 μm. See also Figure S3.

mechanoreceptive nerve fibers and their associated terminal Schwann cells (Li and Ginty, 2014). Traced cells at the free nerve endings of nociceptive fibers showed an atypical morphology, with the soma localized in the upper part of the dermis, close to the epidermis, while a dense network of cytoplasmic protrusions penetrated the dermis and epidermis and followed the path of nerve terminals (Figure 3G). These cytoplasmic protrusions are often in close contact with blood vessels in the dermis (Figure 3H). These cells are likely to correspond to the teloglia, which was once described by Cauna, but not further investigated (Cauna, 1973). Interestingly, while some traced cells associated with the lanceolate endings expressed the progenitor/stem cell marker nestin, this was not the case for any of those associated with the free nerve endings (Figure 3I).

In the adult skin, the distribution and immunohistological signature of traced cells along the neuronal cutaneous network were comparable to that of newborns (Figures S4A–S4C). We further characterized adult BC derivatives in the hypodermis using electron microscopy. For this purpose, we used $Prss56^{Cre/+},R26^{lacZ}$ animals, where Cre recombination leads to permanent expression of β-galactosidase, which can convert the Bluogal substrate into electron-dense precipitates (Maro et al., 2004). Analysis of subcutaneous nerves confirmed that the majority of the labeled cells were non-myelinating Schwann cells (Figure S4D), but also identified a few myelinating Schwann cells (Figure S4D), as observed in the newborn (Figure 3B), and endoneurial fibroblasts, characterized by the absence of basal lamina (Figures S4D and S4E).

Together, our data indicate that BC cell derivatives in neonatal and adult skin consist mainly of Schwann cells, most of them non-myelinating, and some endoneurial fibroblasts. Among the Schwann cells, some are associated with the dermal nerve fibers and others with nerve terminals, either lanceolate or free endings.
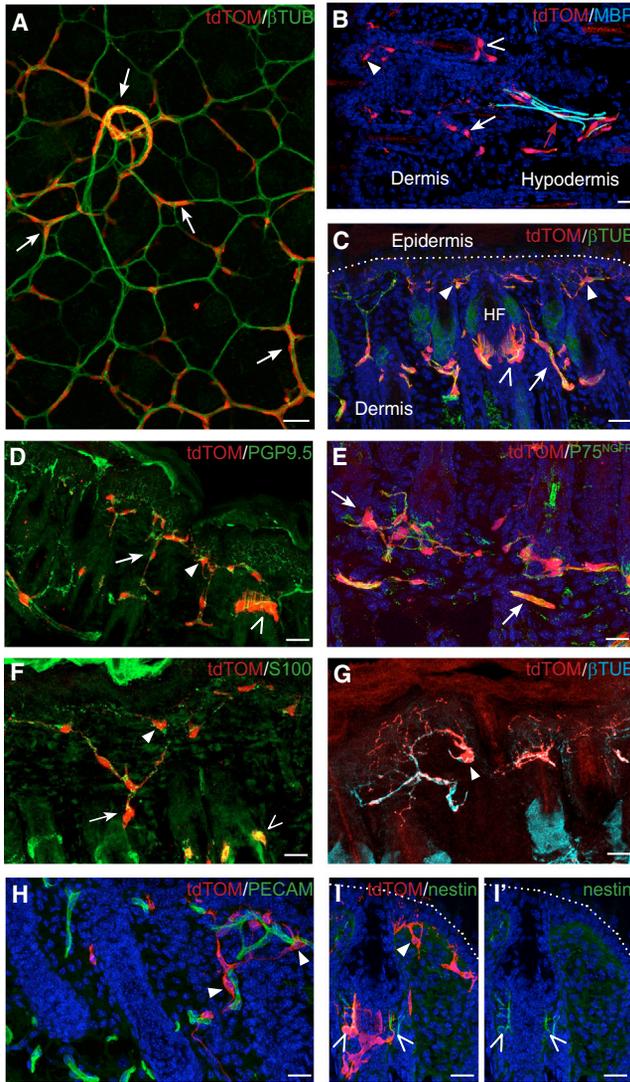
Figure 3. Identities of BC Derivatives in the Neonatal Skin

(A) Whole-mount immunostaining of newborn skin from *Prss56*[Cre/+], *R26*[tdTom] animals for tdTOM and βIII-tubulin, viewed from the hypodermal side. Most traced cells are in contact with the subcutaneous or dermal nerves (arrows).

(B–I) Transverse sections of the skin from *Prss56*[Cre/+],*R26*[tdTom] newborn animals labeled with the indicated antibodies. In the hypodermis, traced cells are associated with the cutaneous nerves and some express the myelin marker MBP (B, red arrow). In the dermis, tdTOM-positive cells are localized along βIII-tubulin-positive axons (C) and PGP9.5-positive terminal nerve fibers (D), and they express the NC stem cell/immature glial marker P75[NGFR] (E) and the Schwann cell marker S100 (F), but not the myelin marker MBP (B, white arrow and open and closed arrowheads). These Schwann-like cells are associated with dermal nerves (A and C–F, arrows), free nerve endings (C, D, and F–I, closed arrowheads), or lanceolate endings of hair follicles (C, D, F, and I, open arrowheads). The cells associated with free nerve endings are highly ramified and are often in direct contact with blood vessels (G and H, arrowheads). Some of the traced

Dermal BC Derivatives Can Be Propagated in Sphere Cultures and Are Multipotent

NC-derived progenitor/stem cells that express P75[NGFR] and SOX10 have been described in the mouse and human skin (Wong et al., 2006). These characteristics are similar to those of skin BC derivatives (Figure 3E; Figure S3D) and led us to investigate whether some BC derivatives show stem cell-like properties. For this purpose, we performed floating sphere cultures from the back skin of *Prss56*[Cre/+], *R26*[tdTom] newborn mice (Biernaskie et al., 2006; Wong et al., 2006). Numerous floating spheres were observed after 7–10 days in culture and could be propagated for at least 11 passages (Figure 4A). We used our tracing system to monitor BC derivatives over time in these cultures. While tdTOM-positive cells only represented 0.1% of the cells recovered after skin dissociation, their proportion increased during successive passages to reach approximately 80% of the sphere population at passage 10 (P10) (Figures 4A and 4B).

The rapid increase in the proportion of tdTOM-positive cells during the early passages might reflect either a proliferative advantage of traced cells or a de novo activation of the *Prss56* locus in previously unlabeled cells. *Prss56* expression was not detected by RT-PCR in cells freshly isolated from newborn skin or maintained in sphere culture for two, four, eight and 11 passages (Figure S5A). To avoid a possible dilution of the RT-PCR signal from rare stem cells at early culture stages, we enriched the initial culture in tdTOM-positive stem cells by immuno-panning, taking advantage of the fact that they derive from P75[NGFR]-positive cells (see below). Once again, no *Prss56* expression was observed either immediately after immuno-panning or after 36 hr culture in sphere conditions (Figure S5B). Together, these data are not consistent with de novo activation of *Prss56* in culture conditions and suggest a proliferative advantage for the traced cells. In agreement with this interpretation, immunostaining analysis with the mitotic marker phospho-histone H3 showed that more than 97% of the floating tdTom-positive cells expressed this marker after 36 hr in culture (Figure S5C), indicating that these cells are highly proliferative.

We next characterized tdTOM-positive cells from spheres. Staining of P2 spheres indicated that tdTOM-positive cells express immature glial/neural stem cell markers, including P75[NGFR], vimentin, fibronectin, nestin, and SOX2, but not the CNS progenitor marker OLIG2 (Figure 4C). Further characterization was performed by RT-PCR on cells isolated from freshly dissociated skin

cells at lanceolate endings express nestin (I and I′, empty arrowheads).
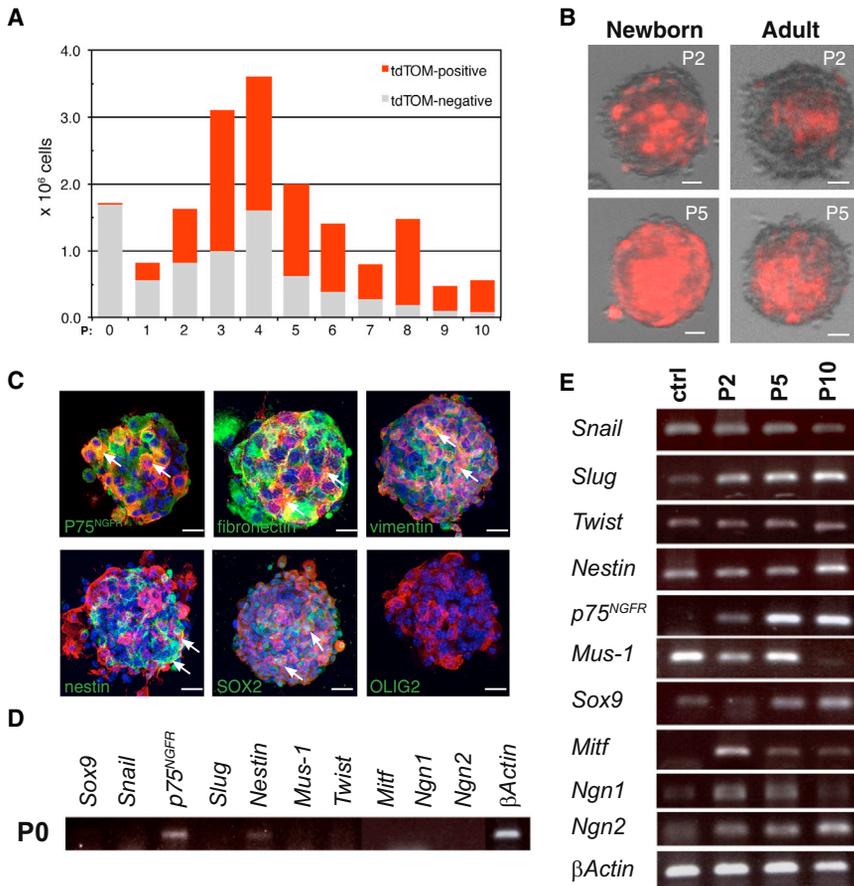
Scale bars, 50 μm. See also Figure S4.

Figure 4. In Vitro Characterization of Skin BC Derivatives

(A) Evolution in the numbers of tdTOM-positive and -negative cells at successive passages (P) in sphere cultures from $Prss56^{Cre/+}, R26^{tdTom}$ newborn skin is shown.

(B) Examples of spheres generated from newborn and adult skin at P2 and P5 show the content in traced cells (red).

(C) Characterization of tdTOM-positive cells (red) from P2 spheres with glial and stem/progenitor markers (green). Arrows point to traced cells positive for the indicated marker.

(D and E) RT-PCR analysis of the expression of NC and stem/progenitor-specific genes in newborn skin cells immediately after dissociation (D) or cultured in sphere-forming medium at the indicated passage (E). In (E), the control (ctrl) corresponds to RNA extracted from the neural tube of E8.5 embryos.

Scale bars, 100 μm (B) and 50 μm (C). See also Figure S5 and Table S1.

(P0) or maintained in sphere culture for two, five, and ten passages. Dissociated cells from back skin expressed $p75^{NGFR}$ and low levels of *nestin* (Figure 4D). Exposure to sphere-forming culture conditions led to increases in the levels of expression of several NC (*Snail*, *Slug*, and *Twist*) and immature cell (*nestin*, $p75^{NGFR}$, and *musashi-1*) markers (Figure 4E), presumably reflecting the increasing proportion of tdTom-positive cells. The spheres also expressed early markers of NC-derived lineages, including chondrocytes (*Sox9*), melanocytes (*Mitf*), and neurons (*Ngn1* and *Ngn2*) (Figure 4E).

We next analyzed the differentiation potential of cultured tdTOM-positive cells. Cells from neonatal $Prss56^{Cre/+}, R26^{tdTom}$ skin were maintained in culture for two or five passages, mechanically dissociated, and cultured for 2 additional weeks in the presence of serum, which promotes their spontaneous differentiation. They were then analyzed according to their morphology and by immunostaining with antibodies against tdTOM and neuronal (βIII-tubulin), Schwann cell (S100), and myofibroblast (SMA) markers. In both P2 and P5 cultures, numerous neurons, myofibroblasts, as well as rare Schwann cells and adipocytes were observed among the

traced population (Figures 5A–5E). We also investigated the response of these dermal BC-derived cells to lineage-specific factors added to the differentiation medium. The addition of forskolin and heregulin greatly enhanced the capacity of spheres to differentiate into Schwann cells (Figure 5F). The addition of stem cell factor (SCF) and endothelin-3 promoted the generation of melanocytes (Figure 5G), while ascorbic acid and bone morphogenetic protein 2 (BMP2) favored the generation of chondrocytes (Figure 5H). These results are consistent with the expression of early markers of NC-derived lineages in spheres (Figure 4E). We also assessed the capacity of spheres to differentiate into a lineage that is not derived from the NC. Inhibition of BMP and Shh signaling enabled the generation of OLIG2-positive immature oligodendocytes, a CNS glial cell type (Figure 5I). Finally, as the spheres obtained from back skin were initially heterogeneous and contained BC derivatives as well as other skin stem cell-like cells, it was important to isolate the BC derivatives as early as possible to investigate their stem cell properties. For this purpose, newborn skin was dissociated and cultured in sphere conditions for 10 days. tdTOM-positive cells were then purified by fluorescence-activated cell sorting (FACS) and cultured
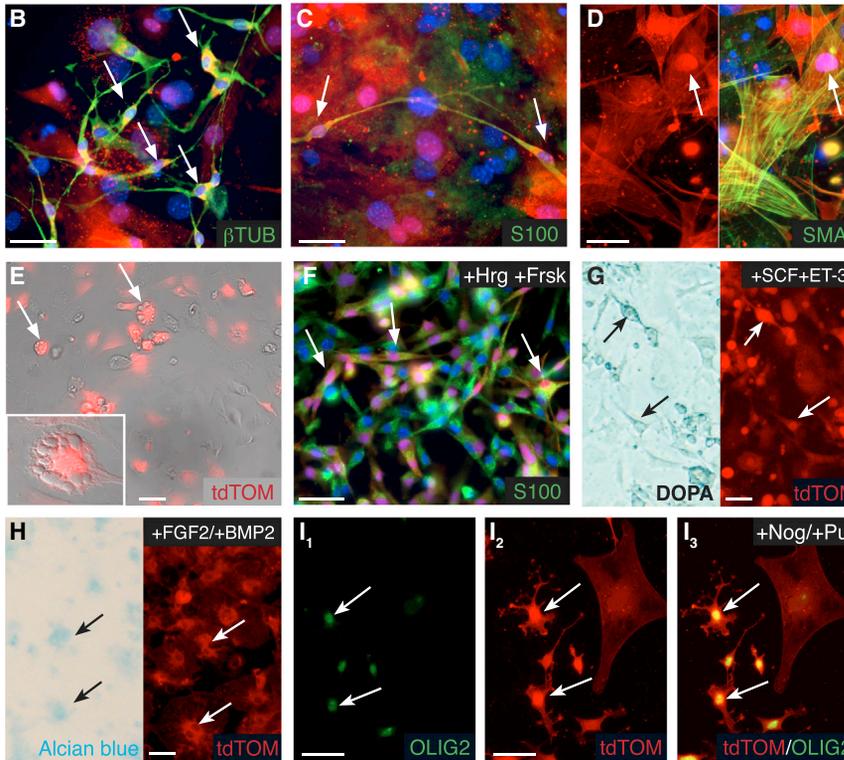
Figure 5. Pluripotency of Skin BC Derivatives In Vitro

(A) Cell type distribution of tdTOM-positive cells from newborn and adult skin cultured in spontaneous differentiation conditions after the indicated passage. Cultures were performed from the total skin population or P75^{NGFR}- or Thy1-positive subpopulation purified by immuno-panning. Cell types were identified by cell morphology and expression of specific markers (see B–E). Approximate distributions are indicated as follows: +, 0.1% to 1%; ++, 1% to 5%; +++, 5% to 15%; and ++++, 15% to 40%.

(B–I) Cell type identification of tdTOM-positive cells from newborn skin cultured in spontaneous (B–E) or induced (F–I) differentiation conditions. Immunolabeling identified the presence of neurons (B, βIII-tubulin positive), Schwann cells (C and F, S100 positive), and myofibroblasts (D, smooth muscle actin [SMA] positive). Cells with morphological features of adipocytes (E), characterized by the presence lipid droplets (inset), also were observed. The proportion of Schwann cells was increased upon the addition of forskolin and heregulins during differentiation (F). DOPA reaction and Alcian blue staining revealed the presence of tdTOM-positive melanocytes (G) and chondroncytes (H) after induced differentiation. Differentiation in the presence of noggin and purformamine led to the formation of immature oligodendrocytes (I$_1$–I$_3$, OLIG2 positive). Arrows point to traced cells expressing the indicated marker. Scale bars, 30 μm.

in sphere conditions. tdTOM-positive cells formed spheres that could be propagated for several passages (Figure S6A) and spontaneously differentiated into NC-derived lineages, including neurons, Schwann cells, and myofibroblasts (Figures S6B–S6D). Together, these results indicate that tdTOM-positive cells from back skin can be propagated in sphere culture, possess a broad differentiation potential in culture, and are plastic in their fate.

Finally, we investigated whether these BC derivatives with stem cell properties are maintained in the adult skin. Traced cells in the adult skin were slightly more abundant (0.6% of the total initial population) than in neonatal skin. Sphere cultures performed with adult skin showed similar proliferation and differentiation properties (Figures 4B and 5A). As skin BC derivatives comprise both glial and fibroblast cells, we wondered whether the stem cells belonged to one or the other population. By magnetic immuno-panning against P75^{NGFR} for immature glial cells

and Thy1 for fibroblasts (Manent et al., 2003), we isolated each cell type, as well as the double-negative population, from newborn skin and performed sphere cultures. Spheres containing numerous traced cells were obtained from both glial and fibroblastic populations, but not from the double-negative fraction. In differentiation conditions, the P75^{NGFR}-positive population gave rise to a similar distribution of cell types as without fractionation, whereas neuronal and glial derivatives were absent from the Thy1-positive population (Figure 5A). To further identify the skin tissue layer housing the stem cells, we performed sphere cultures from the hypodermis of neonatal *Prss56$^{Cre/+}$,R26^{tdTom}* mice after magnetic fractionation with P75^{NGFR} antigens. This fraction failed to form spheres, suggesting that the P75^{NGFR}-positive stem cells were restricted to the dermis, since the epidermis was devoid of traced cells. Together, our results indicate that BC derivatives in neonatal skin include a dermal, P75^{NGFR}-positive
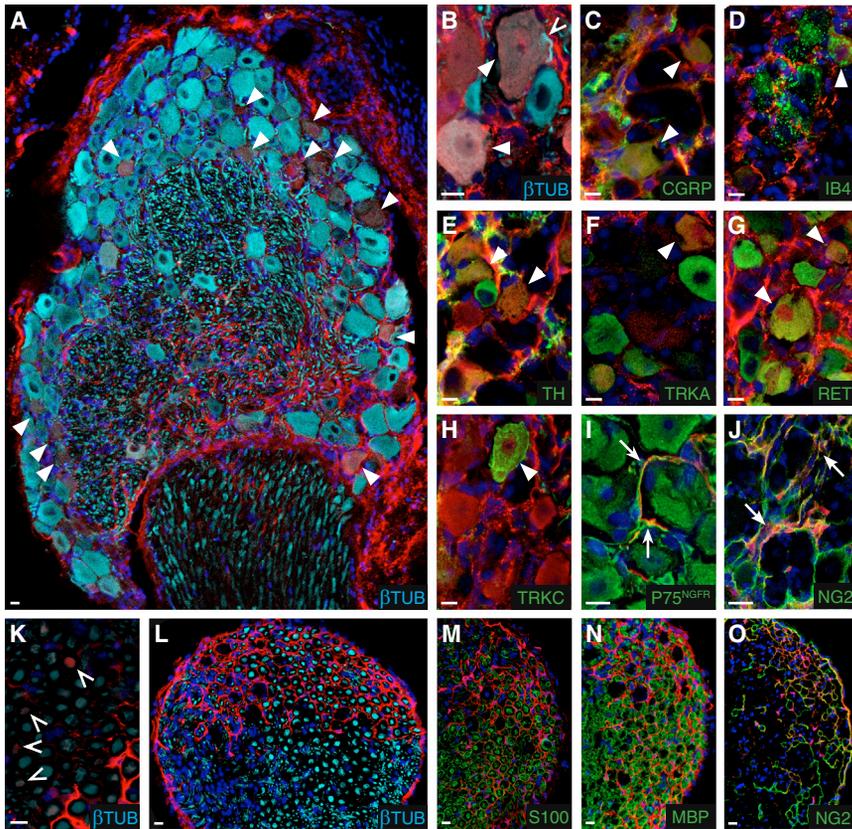
Figure 6. Skin BC Derivatives Give Rise to Various Types of Sensory Neurons upon Transplantation into the DRG

FACS-purified tdTOM-positive cells from skin cultures were injected into the DRGs of nude mice, which were analyzed by immunohistochemistry 30 days later.

(A–J) Transverse sections through the injected DRGs analyzed with antibodies against tdTOM and specific markers of neuronal, glial, or fibroblastic cell types according to the color code. Arrowheads and arrows indicate neuronal and non-neuronal traced cells, respectively.

(K–O) Transverse sections through the spinal nerve attached to the injected DRG. tdTOM-positive axons (empty arrowheads) were observed (K). Numerous traced cells encircled βIII-tubulin-positive axons (L). They were negative for immature (M) and myelinating (N) Schwann cell markers, but expressed NG2 (O), a marker of endo/perineurial fibroblasts.

Scale bars, 10 μm.

stem cell-like population that shows a broad differentiation potential and persists in the adult.

Skin BC Derivatives Grafted into the DRG Efficiently Differentiate into Sensory Neurons

To investigate the in vivo differentiation potential of skin BC derivatives, we first performed transplantations into adult DRGs. Newborn skin was dissociated and cultured in sphere conditions for 10 days. tdTOM-positive cells were then purified by FACS and injected into the L4 or L5 DRG of nude mice (2×10^4 traced cells/DRG). Mice were sacrificed 30 days after grafting and the injected DRGs were analyzed for the presence of tdTOM-positive cells. Of the 30 mice injected, 27 showed numerous tdTOM-positive cells in the injected DRGs. Within the successfully injected DRGs, most traced cells were positive for the neuronal marker βIII-tubulin (Figures 6A and 6B) and represented 12% ± 1.0% of all neurons in the DRG. Traced neurons were further characterized with markers of different categories of mature DRG neurons (Lallemend and Ernfors, 2012) and represented a large array of sensory neurons as follows: peptidergic (CGRP-positive, Figure 6C) and non-peptidergic (binding isolectin B4, Figure 6D) nociceptors; unmyelinated mechanoceptors (tyrosine hydroxylase-positive, Figure 6E); TRKA-positive neurons (Figure 6F), which

include lightly myelinated nociceptors and a subpopulation of peptidergic nociceptors; RET-positive neurons (Figure 6G), which include myelinated mechanoceptors and a subpopulation of peptidergic and non-peptidergic nociceptors; and TRKC-positive neurons (Figure 6H), which include subpopulations of myelinated proprioceptors and mechanoceptors. Furthermore, immunostaining for βIII-tubulin in transverse sections through the dorsal root attached to the injected DRG revealed numerous tdTOM-positive axons (Figure 6K), indicating that at least some of the traced neurons had generated long projections. Together, these data indicate that the grafted cells efficiently differentiate into mature sensory neurons.

Other types of traced cells were observed within the DRG as follows: small, elongated P75^NGFR-positive cells in close contact with neuronal somata, which are glial satellite cells (Figure 6I); cells positive for the proteoglycan NG2 (Figure 6J), which is produced by perineurial and endoneurial fibroblasts in the rat adult sciatic nerve (Morgenstern et al., 2003); and a layer of cells surrounding the DRG, whose identity remains unknown (Figure 6A). Finally, numerous tdTOM-positive cells were observed in the dorsal root and spinal nerve attached to the injected DRG, indicating that injected cells had migrated away from the injection site (Figure 6L). These cells formed a dense network
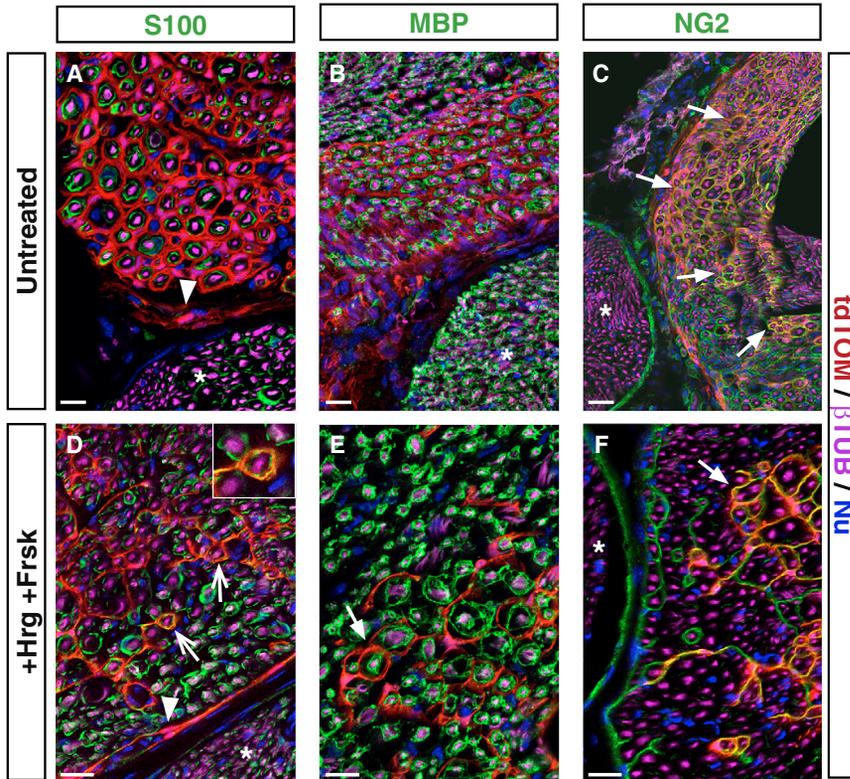
Figure 7. Skin BC Derivatives Give Rise to Peripheral Fibroblasts and Schwann Cells upon Injection into the Injured Sciatic Nerve

Newborn skin BC derivatives were cultured until P1, FACS purified (A–C; untreated) or treated with heregulin/forskolin (D–F; +Hrg+Frsk), and injected into injured sciatic nerves. Transverse sections of the grafted sciatic nerves were analyzed 6 weeks after grafting by immunohisto-chemistry with antibodies against tdTOM and the indicated neuronal, glial, and fibroblastic markers. Arrowheads point to perineurial cells, closed arrows to endo-neurial cells, and open arrows to Schwann cells. Nu, nuclear staining. Ungrafted nerve bundles (asterisks) do not contain tdTOM-positive cells. Scale bars, 50 μm.

around the Schwann cell-axon bundles, and they were negative for immature (S100, Figure 6M) or myelinating (MBP, Figure 6N) Schwann cell markers, but were positive for NG2 (Figure 6O). Therefore, traced cells also differentiate into endo/perineurial-like fibroblasts in the dorsal root and the spinal nerve.

Together, our results indicate that, following injection into adult DRG, skin BC derivatives efficiently colonize the DRG and part of the spinal nerve and give rise to different cell types, including a variety of sensory neurons as well as glial cells and fibroblasts.

Skin BC Derivatives Grafted into Lesioned Peripheral Nerves Give Rise to Endo/Perineurial and Schwann Cells

To investigate whether skin BC derivatives also could differentiate in vivo into Schwann cells when provided with an appropriate environment, we performed transplantations into the cryo-lesioned sciatic nerves of nude mice (Stoll and Müller, 1999). Sciatic nerve lesions are known to enable recruitment of Schwann cells (Jessen et al., 2015). tdTOM-positive cells were prepared as for DRG transplantations and grafted into the lesion site. Six weeks later, numerous traced cells were observed within the lesion site (Figure 6A) as well as in the proximal part of the nerve, indicating that traced cells had efficiently colonized the lesioned nerve.

Analyses of transverse and longitudinal nerve sections indicated that grafted traced cells were not in direct contact with the regenerated axons and were negative for markers for immature (S100, Figure 7A) and myelinating (MBP, Figure 7B) Schwann cells. Most traced cells appeared to wrap single axon/Schwann cell units (Figures 7A and 7B, closed arrows), in a manner similar to endoneurial fibroblasts (Morgenstern et al., 2003). Some traced cells were also at the level of the perineurium (Figure 7A, arrowheads), en-sheathing fascicles composed of axons, their associated Schwann cells, and the surrounding endoneurium. Consistent with these observations, the traced cells were positive for the NG2 marker (Figure 7C). Thus, after transplantation into the injured sciatic nerve, tdTOM-positive cells do not engage into the glial pathway and differentiate preferentially into endo/perineurial-like fibroblasts.

We finally asked whether exposing tdTOM-positive cells to factors promoting a Schwann cell fate prior to transplantation would modify this situation. Skin-derived spheres were maintained for 2 weeks in the presence of forskolin and heregulin, then dissociated and injected into the injured sciatic nerve. Six weeks after transplantation, although most traced cells were NG2-positive fibroblastic cells (Figures 7D–7F), we observed some S100-positive Schwann cells (Figure 7D, open arrows), which had remained immature as they did not express the MBP myelin

marker (Figure 7E). Together, our results indicate that, in the lesioned sciatic nerve environment, grafted BC-derived skin stem cells mainly engage into an endo/perineurial fibroblastic fate, although in vitro treatment with Schwann cell fate-promoting factors redirects some of them toward the glial pathway.

DISCUSSION

This study builds on previous observations that the NC contribution to PNS formation occurs in two waves (Maro et al., 2004), with one population migrating directly to their target locations, while the other makes a stop at the level of the BCs. In contrast to what was previously thought (Maro et al., 2004), we establish that the two waves make similar qualitative contributions in terms of neuronal subtypes in the DRG. Along peripheral nerves of the trunk, the BCs provide the entire proximal Schwann cell nerve root component, as well as a large part of the glia covering the distal parts of skin nerves, whereas the direct NC contribution appears largely restricted to the intermediate part of the nerves. These distinct origins may underlie functional differences between glial populations at different levels along the nerves.

These data have to be considered in the context of recent studies that have shown that embryonic peripheral nerves contain progenitor cells with NC-like potential. Specifically, the early glial components of peripheral nerves, the Schwann cell precursors, possess extensive differentiation capacities as, in addition to Schwann cells (Jessen et al., 2015), they can give rise to melanocytes in the skin (Adameyko et al., 2009), parasympathetic neurons (Dyachuk et al., 2014; Espinosa-Medina et al., 2014), and mesenchymal derivatives in the tooth (Kaukua et al., 2014). However, BC cells appear distinct from these pluripotent glial populations by their location at the PNS/CNS boundary, the expression of specific markers such as Krox20 and Prss56 (Coulpier et al., 2009), and the identity of their derivatives. Furthermore, some BC derivatives maintain their pluripotency in adult tissues, while the pluripotency of Schwann cell precursors is restricted to a specific developmental period.

In the skin, we have shown that BC derivatives give rise to at least three glial populations as follows: Schwann cells (mainly non-myelinating) associated with subcutaneous and dermal nerves, and two types of terminal Schwann cells, associated with lanceolate endings or free nerve endings. Lanceolate endings are specialized sensory organs that detect hair movement (Abraira and Ginty, 2013). They form a palisade structure surrounding the hair follicle and are composed of terminal fibers carrying rapidly adapting low-threshold mechanoreceptors (Aβ, Aδ, and C)

(Abraira and Ginty, 2013). The terminal Schwann cells are involved in the maintenance of the lanceolate complex (Li and Ginty, 2014) and could play a role in calcium signaling (Takahashi-Iwanaga et al., 2008).

Free nerve endings are non-specialized cutaneous sensory receptors that are involved in the perception of touch, pressure, and pain (Abraira and Ginty, 2013). In contrast to their name, free nerve endings also are associated with terminal Schwann cells. Terminal Schwann cells have been studied only by electron microscopy and present a very peculiar morphology, with numerous cytoplasmic protrusions covering the axons at the dermis/epidermis boundary (Cauna, 1973). We provide here a genetic marker that enables optical observations of these cells. Their morphology resembles that of perisynaptic Schwann cells (PSCs), which cap motor nerve terminals at the neuromuscular junction (Balice-Gordon, 1996). PSCs are involved in sensing and modulating synaptic transmission through the specific expression of neurotransmitter receptors and ion channels on their surface (Auld and Robitaille, 2003). Given their similarity with PSCs in terms of terminal location and morphology, we speculate that Schwann cells associated with free nerve endings might play a direct role in depolarizing axon membranes. The $Prss56^{Cre}$ line allows easy identification of these atypical Schwann cells and should facilitate their detailed characterization.

In the dermis, the glial P75^{NGFR}-positive BC derivatives also include a neurogenic and gliogenic stem-like cell population. Multipotent stem-like cell populations have been described previously in the adult trunk skin, associated with the glial and melanocyte lineages and derived from the NC (Wong et al., 2006) or associated with hair follicle dermal cells and derived from the mesoderm (Biernaskie et al., 2009; Jinno et al., 2010). Our results indicate that the BC-derived population constitutes the major, but not single, component of skin stem-like cells detected in these culture conditions, as they represent approximately 80% of the sphere population at late passage. Our work is consistent with recent observations indicating that human adult skin stem cells with neurogenic potential express P75^{NGFR} and can be ascribed to the Schwann cell lineage (Etxaniz et al., 2014). Together, our results establish the precise origin of the large majority of the stem-like cells in the dermis and provide a unique and specific genetic tool for their identification, further study, and manipulation.

Most importantly, grafting experiments establish that this stem cell-like population can efficiently differentiate into various types of mature sensory neurons in the adult DRG. The differentiated neurons survive at least 2 months and many extend long axons in the dorsal root and spinal nerve, although it remains to be determined whether these axons cross the PNS/CNS boundary and establish connections in the spinal cord. Such a neurogenic potential has

never been reported for skin-derived stem cells and it raises the possibility that these cells may manifest an even broader plasticity (e.g., generation of central glia and neurons), if offered the appropriate cellular environment. The fact that these stem cells give rise to a very different distribution of cell types (only endo/perineurial fibroblasts and Schwann cells) upon transplantation into a lesioned sciatic nerve and that they can generate immature oligodendrocytes in vitro is consistent with such a possibility. However, in contrast to the glial character of most traced cells in the dermis, only a small number of Schwann cells are generated after their transplantation into the peripheral nerve. This could reflect differences in the differentiation potentials of BC and newborn skin-traced stem-like cells.

BC derivatives with self-renewal and neurogenic potential also have been identified in the mouse embryonic DRGs (Hjerling-Leffler et al., 2005; Li et al., 2007). In vitro, these stem-like cells re-express NC markers and differentiate efficiently into peripheral sensory neurons (Hjerling-Leffler et al., 2005). Recently, stem/progenitor cells were identified in the adult DRG (Vidal et al., 2015). However, their differentiation might be more restricted as, after transplantation into the lesioned spinal cord, they exclusively generated Schwann cells. It will be interesting to determine whether this population derives from BC cells.

In conclusion, our work opens the way for the detailed analysis of a major population of skin stem cells that are derived from the BCs, have powerful neurogenic potential, and, because of their accessibility, constitute valuable candidates for regenerative medicine. The specific genetic tools developed in the present study should be instrumental for further characterization and manipulation of this promising cell population.

EXPERIMENTAL PROCEDURES

Mouse Lines, Genotyping, and Ethical Considerations

All mouse lines were maintained in a mixed C57BL6/DBA2 background. We used the following alleles or transgenes that were genotyped as indicated in the original publications: $Krox20^{Cre}$ (Voiculescu et al., 2000), $Rosa26^{lacZ}$ (Soriano, 1999), $Rosa26^{tdTom}$ (Madisen et al., 2010), and $Krox20^{lacZ}$ (Schneider-Maunoury et al., 1993). $Prss56^{Cre}$ was generated in this work (see Figure S1). Genotyping was performed by PCR on tail DNA using primers described in Table S1. Day of the plug was considered E0.5. Animals were sacrificed by decapitation (newborn) or cervical dislocation (adult) unless indicated otherwise. All animal manipulations were approved by a French Ethical Committee (Project Ce5/2012/115) and were performed according to French and European Union regulations.

FACS

tdTOM-positive cells were isolated from neonatal skin cell preparations and cultured as floating spheres. Primary spheres were me-

chanically dissociated and the resulting cell suspension (3×10^6 cells/ml) was purified on a FacsVantage (Becton Dickinson) equipped with an argon laser tuned to 561 nm. Dead cells and doublets were excluded by gating on a forward-scatter and side-scatter area versus width. Log RFP fluorescence was acquired through a 530/30 band pass. Internal tdTOM-negative cells served as negative controls for FACS gating. tdTOM-positive cells were sorted directly into culture medium until use in transplantation assays. For verification of the purity of the sorted cells, aliquots of the tdTOM-positive and tdTOM-negative fractions were sorted via FACS again with similar gating parameters and, in parallel, seeded onto coverslips and analyzed by immunohistochemistry with anti-tdTOM antibody.

Transplantations into the DRGs and Sciatic Nerve

Adult nude mice were anesthetized by intra-peritoneal injection of ketamine (Imalgene 500; 0.5 μl/g) and xylazine (Rompun 2%, 0.2 μl/g) before surgery. In addition, local anesthesia (lidocaine) was applied. The tdTOM-positive cells were prepared from neonatal skin, cultured for 10 days in sphere conditions, purified by FACS, and immediately injected. For transplantation into the DRG, the lower lumbar vertebral column was exposed by a midline incision of the skin and fascia, and the right L4 or L5 DRG was exposed via a hemi-laminectomy. A suspension containing 2×10^4 tdTOM-positive cells (10^4 cells/μl) was injected into the DRG. After 1 month, the animals were injected with a lethal dose of ketamine and xylazine and perfused with saline, followed by a fixative solution containing 4% paraformaldehyde (PFA) in PBS. The DRG with the attached nerve roots and spinal nerves was dissected, post-fixed in 4% PFA for 3 hr, and cryoprotected overnight in PBS containing 15% sucrose. Serial 14-μm cryosections were prepared and stored at −80°C until analysis. For transplantation into the sciatic nerve, the nerve was exposed and crushed four times for 10 s with forceps chilled in liquid nitrogen. A suspension containing 10^5 tdTOM-positive cells (5×10^4 cells/μl) was immediately injected into the lesion site as previously described (Stoll and Müller, 1999). After 6 weeks, the animals were sacrificed and the injected sciatic nerves were dissected, fixed in 4% PFA for 3 hr, and cryoprotected overnight. Serial 14-μm cryosections were prepared and stored at −80°C until analysis.

SUPPLEMENTAL INFORMATION

Supplemental Information includes Supplemental Experimental Procedures, six figures, and one table and can be found with this article online at http://dx.doi.org/10.1016/j.stemcr.2015.06.005.

AUTHOR CONTRIBUTIONS

A.G., F.C., P.T., and P.C. designed the experimental paradigm. A.G., F.C., G.G., A.J., G.M., L.R., and P.T. performed the experiments. A.G., F.C., G.G., J.-M.V., P.C., and P.T. analyzed the data. A.G., P.C., and P.T. wrote the paper.

ACKNOWLEDGMENTS

REFERENCES

Abraira, V.E., and Ginty, D.D. (2013). The sensory neurons of touch. Neuron *79*, 618–639.

Adameyko, I., Lallemend, F., Aquino, J.B., Pereira, J.A., Topilko, P., Müller, T., Fritz, N., Beljajeva, A., Mochii, M., Liste, I., et al. (2009). Schwann cell precursors from nerve innervation are a cellular origin of melanocytes in skin. Cell *139*, 366–379.

Auld, D.S., and Robitaille, R. (2003). Perisynaptic Schwann cells at the neuromuscular junction: nerve- and activity-dependent contributions to synaptic efficacy, plasticity, and reinnervation. Neuroscientist *9*, 144–157.

Balice-Gordon, R.J. (1996). Dynamic roles at the neuromuscular junction. Schwann cells. Curr. Biol. *6*, 1054–1056.

Biernaskie, J.A., McKenzie, I.A., Toma, J.G., and Miller, F.D. (2006). Isolation of skin-derived precursors (SKPs) and differentiation and enrichment of their Schwann cell progeny. Nat. Protoc. *1*, 2803–2812.

Biernaskie, J., Paris, M., Morozova, O., Fagan, B.M., Marra, M., Pevny, L., and Miller, F.D. (2009). SKPs derive from hair follicle precursors and exhibit properties of adult dermal stem cells. Cell Stem Cell *5*, 610–623.

Cauna, N. (1973). The free penicillate nerve endings of the human hairy skin. J. Anat. *115*, 277–288.

Coulpier, F., Le Crom, S., Maro, G.S., Manent, J., Giovannini, M., Maciorowski, Z., Fischer, A., Gessler, M., Charnay, P., and Topilko, P. (2009). Novel features of boundary cap cells revealed by the analysis of newly identified molecular markers. Glia *57*, 1450–1457.

Dupin, E., and Sommer, L. (2012). Neural crest progenitors and stem cells: from early development to adulthood. Dev. Biol. *366*, 83–95.

Dyachuk, V., Furlan, A., Shahidi, M.K., Giovenco, M., Kaukua, N., Konstantinidou, C., Pachnis, V., Memic, F., Marklund, U., Müller, T., et al. (2014). Neurodevelopment. Parasympathetic neurons originate from nerve-associated peripheral glial progenitors. Science *345*, 82–87.

Espinosa-Medina, I., Outin, E., Picard, C.A., Chettouh, Z., Dymecki, S., Consalez, G.G., Coppola, E., and Brunet, J.F. (2014). Neurodevelopment. Parasympathetic ganglia derive from Schwann cell precursors. Science *345*, 87–90.

Etxaniz, U., Pérez-San Vicente, A., Gago-López, N., García-Dominguez, M., Iribar, H., Aduriz, A., Pérez-López, V., Burgoa, I., Irizar, H., Muñoz-Culla, M., et al. (2014). Neural-competent cells of adult human dermis belong to the Schwann lineage. Stem Cell Reports *3*, 774–788.

Hjerling-Leffler, J., Marmigère, F., Heglind, M., Cederberg, A., Koltzenburg, M., Enerbäck, S., and Ernfors, P. (2005). The boundary cap: a source of neural crest stem cells that generate multiple sensory neuron subtypes. Development *132*, 2623–2632.

Jessen, K.R., Mirsky, R., and Lloyd, A.C. (2015). Schwann cells: development and role in nerve repair. Cold Spring Harb. Perspect. Biol., a020487.

Jinno, H., Morozova, O., Jones, K.L., Biernaskie, J.A., Paris, M., Hosokawa, R., Rudnicki, M.A., Chai, Y., Rossi, F., Marra, M.A., and Miller, F.D. (2010). Convergent genesis of an adult neural crest-like dermal stem cell from distinct developmental origins. Stem Cells *28*, 2027–2040.

Kaukua, N., Shahidi, M.K., Konstantinidou, C., Dyachuk, V., Kaucka, M., Furlan, A., An, Z., Wang, L., Hultman, I., Ährlund-Richter, L., et al. (2014). Glial origin of mesenchymal stem cells in a tooth model system. Nature *513*, 551–554.

Lallemend, F., and Ernfors, P. (2012). Molecular interactions underlying the specification of sensory neurons. Trends Neurosci. *35*, 373–381.

Le Douarin, N.M., and Dupin, E. (2003). Multipotentiality of the neural crest. Curr. Opin. Genet. Dev. *13*, 529–536.

Li, L., and Ginty, D.D. (2014). The structure and organization of lanceolate mechanosensory complexes at mouse hair follicles. eLife *3*, e01901.

Li, H.-Y., Say, E.H.M., and Zhou, X.-F. (2007). Isolation and characterization of neural crest progenitors from adult dorsal root ganglia. Stem Cells *25*, 2053–2065.

Madisen, L., Zwingman, T.A., Sunkin, S.M., Oh, S.W., Zariwala, H.A., Gu, H., Ng, L.L., Palmiter, R.D., Hawrylycz, M.J., Jones, A.R., et al. (2010). A robust and high-throughput Cre reporting and characterization system for the whole mouse brain. Nat. Neurosci. *13*, 133–140.

Manent, J., Oguievetskaia, K., Bayer, J., Ratner, N., and Giovannini, M. (2003). Magnetic cell sorting for enriching Schwann cells from adult mouse peripheral nerves. J. Neurosci. Methods *123*, 167–173.

Marmigère, F., and Ernfors, P. (2007). Specification and connectivity of neuronal subtypes in the sensory lineage. Nat. Rev. Neurosci. *8*, 114–127.

Maro, G.S., Vermeren, M., Voiculescu, O., Melton, L., Cohen, J., Charnay, P., and Topilko, P. (2004). Neural crest boundary cap cells constitute a source of neuronal and glial cells of the PNS. Nat. Neurosci. *7*, 930–938.

Morgenstern, D.A., Asher, R.A., Naidu, M., Carlstedt, T., Levine, J.M., and Fawcett, J.W. (2003). Expression and glycanation of the NG2 proteoglycan in developing, adult, and damaged peripheral nerve. Mol. Cell. Neurosci. *24*, 787–802.

Nair, K.S., Hmani-Aifa, M., Ali, Z., Kearney, A.L., Ben Salem, S., Macalinao, D.G., Cosma, I.M., Bouassida, W., Hakim, B., Benzina, Z., et al. (2011). Alteration of the serine protease PRSS56 causes angle-closure glaucoma in mice and posterior microphthalmia in humans and mice. Nat. Genet. *43*, 579–584.

Niederländer, C., and Lumsden, A. (1996). Late emigrating neural crest cells migrate specifically to the exit points of cranial branchio-motor nerves. Development 122, 2367–2374.

Schneider-Maunoury, S., Topilko, P., Seitandou, T., Levi, G., Cohen-Tannoudji, M., Pournin, S., Babinet, C., and Charnay, P. (1993). Disruption of Krox-20 results in alteration of rhombomeres 3 and 5 in the developing hindbrain. Cell 75, 1199–1214.

Soriano, P. (1999). Generalized lacZ expression with the ROSA26 Cre reporter strain. Nat. Genet. 21, 70–71.

Stoll, G., and Müller, H.W. (1999). Nerve injury, axonal degeneration and neural regeneration: basic insights. Brain Pathol. 9, 313–325.

Takahashi-Iwanaga, H., Nio-Kobayashi, J., Habara, Y., and Furuya, K. (2008). A dual system of intercellular calcium signaling in glial nets associated with lanceolate sensory endings in rat vibrissae. J. Comp. Neurol. 510, 68–78.

Topilko, P., Schneider-Maunoury, S., Levi, G., Baron-Van Evercooren, A., Chennoufi, A.B., Seitanidou, T., Babinet, C., and Charnay, P. (1994). Krox-20 controls myelination in the peripheral nervous system. Nature 371, 796–799.

Vermeren, M., Maro, G.S., Bron, R., McGonnell, I.M., Charnay, P., Topilko, P., and Cohen, J. (2003). Integrity of developing spinal motor columns is regulated by neural crest derivatives at motor exit points. Neuron 37, 403–415.

Vidal, M., Maniglier, M., Deboux, C., Bachelin, C., Zujovic, V., and Baron-Van Evercooren, A. (2015). Adult DRG stem/progenitor cells generate pericytes in the presence of central nervous system (CNS) developmental cues, and Schwann cells in response to CNS demyelination. Stem Cells 33, 2011–2024.

Voiculescu, O., Charnay, P., and Schneider-Maunoury, S. (2000). Expression pattern of a Krox-20/Cre knock-in allele in the developing hindbrain, bones, and peripheral nervous system. Genesis 26, 123–126.

Wong, C.E., Paratore, C., Dours-Zimmermann, M.T., Rochat, A., Pietri, T., Suter, U., Zimmermann, D.R., Dufour, S., Thiery, J.P., Meijer, D., et al. (2006). Neural crest-derived cells with stem cell features can be traced back to multiple lineages in the adult skin. J. Cell Biol. 175, 1005–1015.

Zujovic, V., Thibaud, J., Bachelin, C., Vidal, M., Coulpier, F., Charnay, P., Topilko, P., and Baron-Van Evercooren, A. (2010). Boundary cap cells are highly competitive for CNS remyelination: fast migration and efficient differentiation in PNS and CNS myelin-forming cells. Stem Cells 28, 470–479.

Zujovic, V., Thibaud, J., Bachelin, C., Vidal, M., Deboux, C., Coulpier, F., Stadler, N., Charnay, P., Topilko, P., and Baron-Van Evercooren, A. (2011). Boundary cap cells are peripheral nervous system stem cells that can be redirected into central nervous system lineages. Proc. Natl. Acad. Sci. USA 108, 10714–10719.